

Tridentate [N,N,O] Schiff-base group 4 metal complexes: Synthesis, structural characterization and reactivity in olefin polymerization

Gino Paolucci^{a,*}, Alessandra Zanella^a, Laura Sporni^a,
Valerio Bertolasi^b, Mina Mazzeo^c, Claudio Pellecchia^{c,*}

^a Dipartimento di Chimica, Università Ca' Foscari, Dorsoduro 2137, I-30123 Venezia, Italy

^b Dipartimento di Chimica e Centro di Strutturistica Diffraattometrica, Università di Ferrara, I-44100 Ferrara, Italy

^c Dipartimento di Chimica, Università di Salerno, Via S. Allende, I-84081 Baronissi (SA), Italy

Received 26 April 2006; accepted 17 May 2006

Available online 10 July 2006

Abstract

New complexes LTiCl_3 (**1**), LZrCl_3 (**2**) and LHfCl_3 (**3**) ($\text{L} = (E)\text{-}2\text{-tert-butyl-}6\text{[(quinoline-8-ylimino)methyl]phenolate}$) have been synthesized and fully characterized by multinuclear NMR, mass spectrometry and X-ray diffractometry. The three isostructural complexes show distorted octahedral geometries. Complexes **1–3** were tested as catalysts for ethylene polymerization under a variety of experimental conditions. Reasonable productivities were achieved after activation by methylaluminoxane (MAO) under moderate temperature and pressure conditions (e.g., 50 °C and 6 atm). Complexes **1–3** were also tested as precatalysts for the polymerization of propene. Interestingly, polymerization by **1**-MAO at -20°C afforded an isotactic polypropylene containing 5% isolated regioirregular units in *threo* configuration. This very unusual microstructure implicates that both primary and secondary monomer insertions occur with the same enantioface selectivity, at variance with what is observed in the case of metallocene catalysts.

© 2006 Elsevier B.V. All rights reserved.

Keywords: Titanium; Zirconium; Hafnium; Polyethylene; Polypropylene; Phenoxyimine catalysts

1. Introduction

Although olefin polymerization catalysis can be considered a mature area, the search for new classes of catalysts is continuing in both academic and industrial laboratories, the driving force being the opportunity to explore patent-free areas and to extend the family of polymer and especially copolymer products. Research interest has been directed in the last years toward the design of new cyclopentadienyl-free complexes of both early and late transition metals [1,2]. Among these “post-metallocene” catalysts, complexes of a variety of metals bearing salicylaldiminato-type ligands emerged for their performances [3–10]. In particular, bis(phenoxyimine) group 4 metal complexes developed by Fujita et al. showed ethylene polymerization activities comparable or higher than those of metallocenes [11,12] and peculiar behaviour like living polymerization and

syndiotactic specific polymerization of propene [13–18]. Also, phenoxyimine Ni(II) complexes discovered by Grubbs and co-workers provided neutral ethylene polymerization catalysts not requiring aluminum or boron activators, showing high activity and increased tolerance versus polar species [19].

In this paper, we report the synthesis, the characterization and the performances in the polymerization of ethylene and propene of octahedral LMCl_3 complexes ($\text{M} = \text{Ti, Zr, Hf}$; $\text{L} = (E)\text{-}2\text{-tert-butyl-}6\text{[(quinolin-8-ylimino)methyl]phenolate}$).

While this work was in progress, closely related titanium and zirconium compounds have been reported in a patent as catalysts for olefin polymerization [20].

2. Experimental

2.1. General procedures

All manipulations were carried out under a purified nitrogen atmosphere by using a glove-box apparatus MBraun G200 working at 1 ppm O_2 and <1 ppm H_2O . The commercially available

* Corresponding authors. Tel.: +39 089965423; fax: +39 089965296.
E-mail address: cpellecchia@unisa.it (C. Pellecchia).

solvents, tetrahydrofuran, toluene and *n*-hexane, diethyl ether were distilled from LiAlH₄ and then from sodium benzophenone ketyl under nitrogen. Dichloromethane was distilled over CaH₂. Chlorobenzene was distilled over CaH₂. Deuterated toluene-*d*₈, was dried over Na/K alloy and collected by tow cycles. CD₂Cl₂ and CDCl₃ were dried over CaH₂ and collected by tow cycles. TiOC₂H₅, 3-*tert*-butyl-salicylaldehyde and 8-amine-quinoline, ZrCl₄·2THF, TiCl₄·2THF, HfCl₄ (Aldrich) were used as received. Methylaluminoxane (MAO, Euricem) was purchased as a 10 wt% solution in toluene and used as received. The reagents were purchased from Aldrich Chemical Company. Polymerization grade propene and ethylene (SON, 99%) were used without further purification.

2.2. Analysis methods

NMR spectra were recorded on a Bruker Avance 300 or a Varian Unity 400 spectrometers. Chemical shifts (ppm) for ¹H and ¹³C spectra were internally referenced to the residual undeuterated solvent resonances and related to tetramethylsilane ($\delta=0$ ppm). Mass spectrometric data were collected on a Thermo-Finnigan Trace MS Mass Spectrometer by direct inlet (E.I. 70 eV, $T_{\text{source}}=200$ °C, $T_{\text{probe}}=120$ °C). All the fragment assignments have been done by comparison of the calculated and experimental clusters.

¹³C NMR spectra of polymers were recorded on a AM Bruker 300 MHz spectrometer in 1,1,2,2-tetrachloroethane-*d*₂ (C₂D₂Cl₄, TCDE) and referenced versus hexamethyldisiloxane (HMDS) at 100 °C.

The polymer samples were dissolved in TCDE in a 5 mm o.d. tube by heating on a flame.

Molecular weight and molar mass distribution of polymers were measured by gel-permeation chromatography (GPC). GPC measurements were performed on PL-GPC210 with PL-gel Mixed A columns, RALLS detector (precision detector, PD2040 at 800 nm), H502 Viscometer (Viscotek), refractive detector and DM400 data manager (Viscotek). Every value is the average of two independent measurements.

2.3. Complex synthesis

2.3.1.

(*E*)-3-*tert*-butyl-6-[(quinolin-8-ylimino)methyl]phenol (**LH**)

To a solution of 3-*tert*-butyl-2-salicylaldehyde (0.83 mL, 4.85 mmol) in anhydrous methanol (50 mL) 8-aminoquinoline (0.70 g, 4.85 mmol) dissolved in anhydrous methanol (30 mL) was added under nitrogen atmosphere, and in the presence of molecular sieves (4 Å) and anhydrous Na₂SO₄ (5 g). The reaction mixture was left to react under reflux for 15 h, and then filtered and the solvent eliminated under vacuum to give an orange oily product, which was crystallized from *n*-hexane (1.40 g, 95% yield).

Anal. calcd. for C₂₀H₂₀N₂O: C, 78.66; H, 6.93; N, 9.17%. Found: C, 78.45; H, 6.65; N, 9.35.

¹H NMR (CD₂Cl₂, 300 MHz, δ (ppm), J (Hz)): 14.27 (s, 1H, OH), 9.02 (d, $J=7.2$, 1H, quinoline-2), 8.94 (s, 1H, CH=N-), 8.22 (d, ³ $J_{\text{H-H}}=7.1$, 1H, quinoline-3), 7.75 (d, ³ $J_{\text{H-H}}=6.6$,

1H, 1H, quinoline-4 or -6), 7.59 (t, ³ $J_{\text{H-H}}=7.3$, H1, quinoline-2), 7.49–7.28 (m, 4H, quinoline-4 or -6, quinoline-5, phenyl-8, phenyl-10), 6.9 (t, ³ $J_{\text{H-H}}=7.6$, 1H, phenyl-9), 1.5 (s, 9H, C(CH₃)₃).

¹³C NMR (CD₂Cl₂, 75 MHz, δ (ppm)): 166.5 (C10), 161.67 (C16), 150.8 (C1), 146.4 (C9), 142.7 (C5), 138.2 (C15), 136.41 (C3), 131.2 (C12), 130.8 (C14), 129.6 (C4), 127.0 (C7), 126.3 (C8), 122.0 (C2), 119.9 (C6), 118.5 (C11), (C13), 35.6 (C17), 29.8 (C18).

2.3.2. LTiCl₃ (**1**)

To a solution of the ligand LH (0.550 g, 1.81 mmol) in THF (30 mL) a solution of TiOC₂H₅ (0.128 mL, 1.81 mmol) in THF (5 mL) was added drop wise at -50 °C under magnetic stirring. The temperature was then raised up to room temperature and the mixture left to react for two hours affording an orange suspension (TIL). To a solution of TiCl₄·2THF (0.604 g, 1.81 mmol) in THF (50 mL) the suspension of the thallium salt of the ligand (TIL) (1.064 g, 1.81 mmol) in THF (35 mL) was added drop wise in 30 min at -50 °C. The reaction temperature was raised up to room temperature and the mixture was left to react for 15 h. TiCl₄ was separated by centrifugation and the volume of the red solution reduced under vacuum to 40 mL. By addition of *n*-hexane (20 mL) a red microcrystalline compound precipitated (0.646 g, 78% yield). Red crystals suitable for X-ray analysis were obtained by recrystallization from CH₂Cl₂/*n*-hexane (1:1).

Anal. calcd. for C₂₀H₁₉N₂O₂TiCl₃: C, 52.49; H, 4.18; N, 6.12; Cl, 23.24. Found: C, 52.35; H, 4.05; N, 6.25; Cl, 23.65.

Mass spectrometric data (E.I. 70 eV, $T_{\text{probe}}=120$ °C, m/z): 456 [M]⁺, 421 [M-Cl]⁺, 370 [M-2Cl-O]⁺.

¹H NMR (CD₂Cl₂, 300 MHz, δ (ppm), J (Hz)): 9.79 (d, 1H, ³ $J_{\text{HH}}=5.0$, H-1), 9.09 (s, 1H, H-10), 8.61 (d, 1H, ³ $J_{\text{HH}}=8.3$, H-3), 8.08 (d, 1H, ³ $J_{\text{HH}}=7.8$, H-8), 8.07 (d, 1H, ³ $J_{\text{HH}}=8.2$, H-6), 7.88 (dd, 1H, ³ $J_{\text{HH}}=5.0$, ³ $J_{\text{HH}}=8.3$, H-2), 7.86 (t, 1H, ³ $J_{\text{HH}}=8.3$, H-7), 7.78 (d, 1H, ³ $J_{\text{HH}}=7.8$, H-14), 7.67 (d, 1H, ³ $J_{\text{HH}}=7.8$, H-12), 7.26 (t, 1H, ³ $J_{\text{HH}}=7.8$, H-13), 1.63 (s, 9H, H-18).

¹³C{¹H} NMR (CD₂Cl₂, 75 MHz, δ (ppm)): 159.4 (C10), 152.3 (C1), 140.5 (C3), 136.0 (C14), 134.7 (C12), 129.3 (C7), 128.9 (C6), 125.1 (C2), 123.9 (C13), 117.5 (C8), 35.3 (C17), 29.8 (C18).

2.3.3. LZrCl₃ (**2**)

Following the previous preparation for the titanium complex, a yellow microcrystalline compound was obtained (85% yield). Crystals suitable for X-ray analysis were obtained by recrystallization by CH₂Cl₂/*n*-hexane (1:1).

Anal. calcd. for C₂₀H₁₉N₂OZrCl₃: C, 47.95; H, 3.82; N, 5.59; Cl, 21.23. Found: C, 47.80; H, 3.70; N, 5.65; Cl, 21.45.

Mass spectrometric data (E.I. 70 eV, $T_{\text{probe}}=120$ °C, m/z): 500 [M]⁺, 465 [M-Cl]⁺, 450 [M-CH₃]⁺.

¹H NMR (CD₂Cl₂, 300 MHz, δ (ppm), J (Hz)): 9.85 (dd, 1H, ³ $J_{\text{H-H}}=5.0$, ⁴ $J_{\text{H-H}}=1.1$, H-2), 9.17 (s, 1H, H-10), 8.69 (dd, 1H, ³ $J_{\text{H-H}}=8.3$, ⁴ $J_{\text{H-H}}=1.1$, H-3), 8.16 (d, 1H, ³ $J_{\text{H-H}}=8.0$, H-8), 8.09 (d, 1H, ³ $J_{\text{H-H}}=8.1$, H-6), 7.91 (m, 2H, H-2 + H-7), 7.79 (dd, 1H, ³ $J_{\text{H-H}}=7.8$, ⁴ $J_{\text{H-H}}=1.4$, H-14), 7.65 (dd, 1H, ³ $J_{\text{H-H}}=7.8$,

$^4J_{\text{H-H}} = 1.4$, H-12), 7.18 (t, 1H, $^3J_{\text{H-H}} = 7.8$, H-13), 1.59 (s, 9H, H-18).

$^{13}\text{C}\{^1\text{H}\}$ NMR (CD_2Cl_2 , 75 MHz, δ (ppm)): 164.2 (C10), 159.8 (qC16), 150.4 (C-1), 142.9 (qC5), 141.8 (C-3), 136.0 (C14), 134.7 (C12), 129.3 (C7), 128.9 (C6), 125.1 (C2), 123.9 (C13), 117.5 (C8), 35.6 (C17), 29.8 (C18).

2.3.4. LHfCl_3 (3)

Following the previous preparation for the titanium complex, a yellow microcrystalline compound was obtained (80% yield). Crystals suitable for X-ray analysis were obtained by recrystallization by $\text{CH}_2\text{Cl}_2/n$ -hexane (1:1).

Anal. calcd. for $\text{C}_{20}\text{H}_{19}\text{N}_2\text{OHfCl}_3$: C, 40.84; H, 3.25; N, 4.76; Cl, 18.08. Found: C, 40.35; H, 3.05; N, 4.50; Cl, 17.80.

Mass spectrometric data (E.I. 70 eV, $T_{\text{probe}} = 120^\circ\text{C}$, m/z): 587 $[\text{M}]^+$, 552 $[\text{M}-\text{Cl}]^+$, 572 $[\text{M}-\text{CH}_3]^+$.

^1H NMR (CD_2Cl_2 , 300 MHz, δ (ppm), J (Hz)): 9.49 (dd, 1H, $^3J_{\text{HH}} = 5.0$, $^4J_{\text{HH}} = 1.5$, H-1), 9.14 (s, 1H, H-10), 8.67 (dd, 1H, $^3J_{\text{HH}} = 8.4$, $^4J_{\text{HH}} = 1.5$, H-3), 8.12 (d, 1H, $^3J_{\text{HH}} = 8.0$, H-8), 8.05 (d, 1H, $^3J_{\text{HH}} = 8.1$, H-6), 7.90 (dd, $^3J_{\text{HH}} = 5.0$, $^4J_{\text{HH}} = 8.4$, H-2), 7.88 (t, 1H, $^3J_{\text{HH}} = 8.1$), 7.78 (dd, 1H, $^3J_{\text{HH}} = 7.7$, $^4J_{\text{HH}} = 1.7$, H-14), 7.59 (dd, 1H, $^3J_{\text{HH}} = 7.8$, $^4J_{\text{HH}} = 1.7$, H-12), 7.09 (t, 1H, $^3J_{\text{HH}} = 7.7$, H-13), 1.55 (s, 9H, H-18).

$^{13}\text{C}\{^1\text{H}\}$ NMR (CD_2Cl_2 , 75 MHz, δ (ppm)): 164.6 (C10), 150.8 (C1), 142.0 (C3), 140.4 (C15), 137.0 (C14), 135.5 (C12), 129.5 (C7), 129.0 (C6), 123.6 (C2), 122.4 (C13), 118.5 (C8), 35.4 (C17), 29.7 (C18).

2.3.5. Crystal structure determinations

The crystal data for the compounds **1–3** were collected using a Nonius Kappa CCD diffractometer with graphite monochromated Mo $\text{K}\alpha$ radiation. The data sets were integrated with the Denzo-SMN package [21] and corrected for Lorentz, polariza-

tion and absorption effects (SORTAV [22]). The structures were solved by direct methods (SIR97 [23]) and refined using full-matrix least squares with all non-hydrogen atoms anisotropic and hydrogens included on calculated positions, riding on their carrier atoms. The crystals of compound **3** contain two molecules of tetrahydrofuran *per* molecule of complex.

All calculations were performed using SHELXL-97 [24] and PARST [25] implemented in WINGX [26] system of programs. The crystal data and refinement parameters are summarized in Table 1.

2.3.6. Olefin polymerizations

High pressure polymerizations were performed in a glass reactor (500 cm^3) equipped with a mechanical stirrer and a temperature probe. The reaction vessel was first conditioned under dynamic vacuum at polymerization temperature and then charged with a desired amount of MAO, or $\text{Al}(\text{i}^t\text{Bu})_3$ in the proper solvent. The solvent was thermostated to the required polymerization temperature and stirred (600 rpm), then the ethylene gas feed was started. Polymerization was initiated by adding a solution of a complex in the same solvent (except when otherwise indicated) into the reactor. After the prescribed time the autoclave was vented and the polymerization mixture was poured into acidified ethanol. The precipitated polymer was recovered by filtration, dried (80 $^\circ\text{C}$, vacuum oven, overnight) and weighed.

3. Results and discussion

3.1. Syntheses of the Ti(IV), Zr(IV) and Hf(IV) complexes

The phenoxyimine ligand, (*E*)-2-*tert*-butyl-6-[(quinolin-8-ylimino)methyl]phenol (**LH**), was synthesized in high yield

Table 1
Crystal data

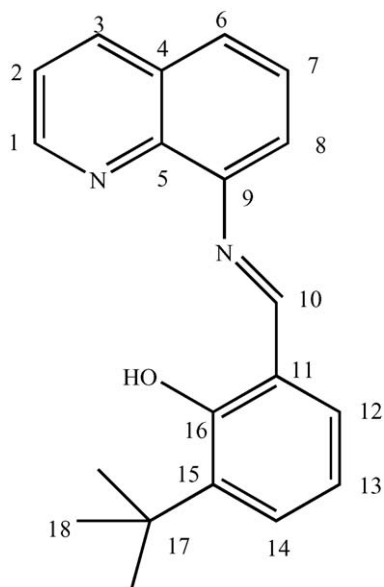
Compound	1	2	3
Formula	$\text{C}_{20}\text{H}_{19}\text{Cl}_3\text{N}_2\text{OTi}$	$\text{C}_{20}\text{H}_{19}\text{Cl}_3\text{N}_2\text{OZr}$	$\text{C}_{20}\text{H}_{19}\text{Cl}_3\text{N}_2\text{OHf}\cdot 2\text{C}_4\text{H}_8\text{O}$
<i>M</i>	457.62	500.94	732.42
System	Monoclinic	Monoclinic	Triclinic
Space group	$P 2_1/n$	$P 2_1/n$	$P -1$
<i>a</i> (Å)	7.0836(2)	8.2801(2)	9.5472(2)
<i>b</i> (Å)	16.5507(5)	16.2623(4)	10.6079(3)
<i>c</i> (Å)	17.9779(7)	15.2613(4)	15.5426(4)
α ($^\circ$)	90	90	96.492(1)
β ($^\circ$)	97.552(1)	90.594(1)	98.214(1)
γ ($^\circ$)	90	90	100.038(2)
<i>U</i> (Å ³)	2089.4(1)	2054.9(1)	1441.24(7)
<i>Z</i>	4	4	2
<i>D_c</i> (g cm ⁻³)	1.455	1.619	1.688
μ (cm ⁻¹)	8.05	9.38	39.29
<i>T</i> (K)	150	295	120
$\theta_{\text{min}}-\theta_{\text{max}}$ ($^\circ$)	2.3–27.0	3.7–28.0	2.7–28.0
Unique refl.ns	4529	4912	6940
<i>R</i> _{int}	0.072	0.125	0.111
Obs. refl.ns; $I > 2\sigma(I)$	3199	3957	5976
<i>R</i> (obs. refl.ns)	0.0795	0.0538	0.0387
<i>wR</i> (all refl.ns)	0.1917	0.1255	0.0919
<i>S</i>	1.162	1.045	1.039
$\Delta\rho_{\text{max}}; \Delta\rho_{\text{min}}$ (e Å ⁻³)	1.32; -0.555	0.98; -1.00	2.41; -1.56

(95%) by the condensation of 3-*tert*-butyl-salicylaldehyde with 8-amine-quinoline, according to the literature method [6]. The reaction of the ligand with TlOC_2H_5 followed by reaction of the thallium salt of the ligand with MCl_4 ($\text{M} = \text{Ti}, \text{Zr}, \text{Hf}$) in THF afforded suspensions from which, after filtering off the TlCl precipitate, red (Ti) or yellow (Zr, Hf) clear solutions resulted. The volume of the solutions was reduced under vacuum to about 10 mL. By addition of *n*-hexane red (Ti) or yellow (Zr, Hf) microcrystalline products were obtained in good yields ($\geq 80\%$).

3.2. NMR characterization of the complexes 1–3

The NMR study of the complexes 1–3 (^1H , ^{13}C , HMQC, HMBC, COSY, NOESY experiments) allowed the complete assignment of all the protons and carbon atoms (in some cases excluding quaternary carbons) following the numbering of the protons and carbon atoms in Scheme 1. Here, we discuss the assignments for the Hf complex, 3. The assignments for the complexes 1 and 2 have been made following the same reasoning.

On the basis of their chemical shifts the singlets at δ 1.55 and 9.14 must be assigned to the methyl protons of the *tert*-butyl group (H18) and to the proton of the $-\text{CH}=\text{N}-$ group (H10), respectively. The NOE interaction with the *tert*-butyl group (H18) allowed to assign the doublet of doublets at δ 7.78 to the H14 hydrogen. By COSY experiment the triplet at δ 7.09 and the doublet of doublets at δ 7.59 were assigned to the H13 and H12 protons, respectively. The NOE interactions with the iminic hydrogen (H10) confirmed this assignment and allowed to identify the H8 proton (doublet centred at δ 8.12). On the basis of the assignment of H8, the triplet at δ 7.88 and the doublet at δ 8.05 must be assigned to H7 and H6, respectively. The signal at δ 9.49, a doublet of doublets, was assigned to the proton (H1) adjacent to the quinoline nitrogen atom. From the multiplicity and COSY experiment (scalar coupling) the signals (doublets



Scheme 1.

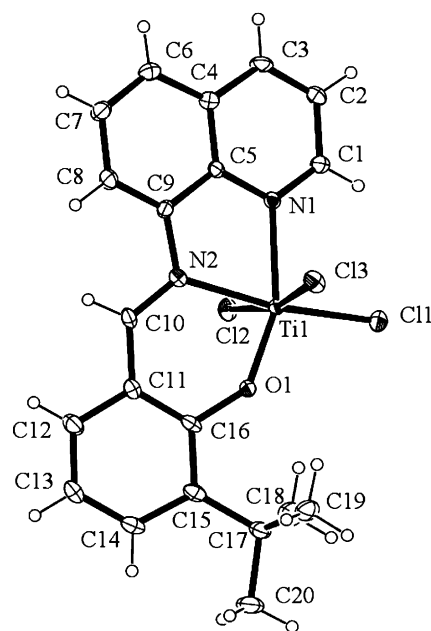


Fig. 1. An ORTEP view of the titanium complex 1 showing thermal ellipsoids at 40% probability.

of doublets) at δ 7.90 and 8.67 were assigned to the protons H2 and H3, respectively. All the experimental coupling constants are in agreement with the assignments. The carbon signals were assigned by HMQC and HMBC experiments.

3.3. X-ray crystal structures of 1–3

ORTEP [27] views of complexes 1–3 are shown in Figs. 1–3. Selected interatomic distances and angles are given in Table 2. The three complexes are isostructural. The overall geometry around the central metal (Ti, Zr or Hf) atom can be described as

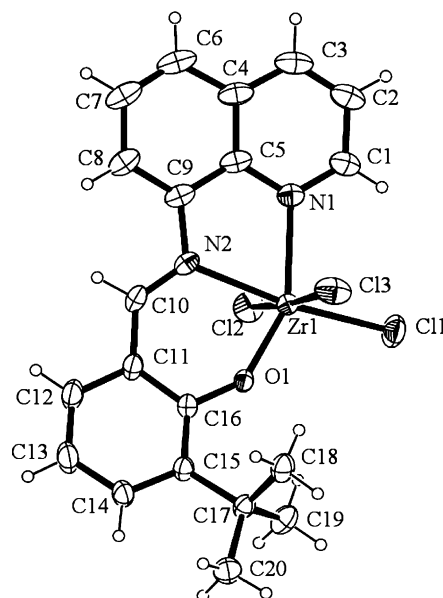


Fig. 2. An ORTEP view of the zirconium complex 2 showing thermal ellipsoids at 40% probability.

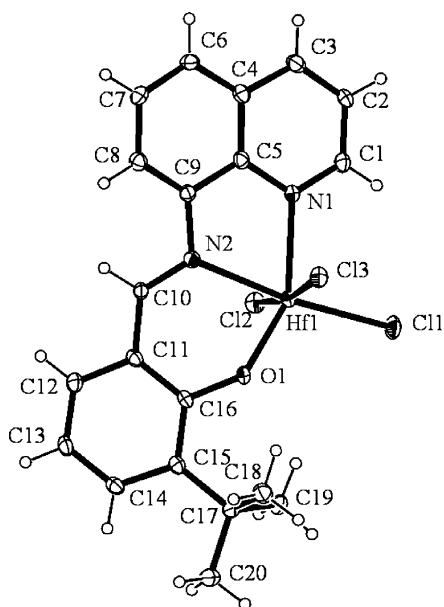


Fig. 3. An ORTEP view of the hafnium complex **3** showing thermal ellipsoids at 40% probability.

a distorted octahedral where the tridentate ligand is bonded to the metal through two neutral nitrogens, N1 from the quinoline ring and N2 from the imino group, and the oxygen O1 from the phenolate group. The other three sites are occupied by three chloride ligands, which are meridionally arranged.

Table 2
Selected bond distances (Å) and angles (°) for compounds **1–3**

	1, M = Ti	2, M = Zr	3, M = Hf
M1–Cl1	2.292(2)	2.429(1)	2.415(1)
M1–Cl2	2.341(2)	2.444(1)	2.431(1)
M1–Cl3	2.302(2)	2.433(1)	2.438(1)
M1–O1	1.797(4)	1.934(2)	1.946(2)
M1–N1	2.190(5)	2.287(3)	2.280(4)
M1–N2	2.169(5)	2.329(3)	2.277(4)
O1–C16	1.356(8)	1.340(4)	1.346(4)
N2–C9	1.423(8)	1.428(5)	1.429(6)
N2–C10	1.299(8)	1.296(5)	1.293(5)
C10–C11	1.445(9)	1.442(5)	1.446(1)
C11–M1–Cl2	90.65(7)	89.37(4)	90.71(4)
C11–M1–Cl3	95.20(7)	88.31(5)	92.41(4)
C11–M1–O1	105.2(2)	109.89(7)	108.10(9)
C11–M1–N1	95.9(1)	100.59(9)	100.5(1)
C11–M1–N2	169.2(1)	169.50(8)	171.6(1)
Cl2–M1–Cl3	167.52(8)	173.69(4)	170.50(4)
Cl2–M1–O1	92.4(1)	95.78(8)	93.33(9)
Cl2–M1–N1	83.6(1)	88.65(9)	86.0(1)
Cl2–M1–N2	83.2(1)	84.27(8)	86.0(1)
Cl3–M1–O1	96.7(1)	90.53(8)	94.23(9)
Cl3–M1–N1	84.9(1)	86.01(9)	84.6(1)
Cl3–M1–N2	89.2(1)	97.14(8)	89.6(1)
O1–M1–N1	158.6(2)	149.2(1)	151.4(1)
O1–M1–N2	84.1(2)	79.1(1)	79.8(1)
N1–M1–N2	74.6(2)	71.0(1)	71.6(1)
M1–O1–C16	141.0(4)	145.4(2)	139.9(3)
M1–N2–C9	116.4(4)	116.6(2)	116.6(3)
M1–N2–C10	124.5(4)	123.6(2)	123.9(3)

In accordance with the different ionic radii of Ti, Zr and Hf, the distances involving Ti1 are significantly shorter than those around Zr1 and Hf1 while the structural parameters in **2** and **3** display comparable values. In complex **1** the Ti–Cl distances in the range 2.292(2)–2.341(2) Å are very similar to those found in TiCl₃-salicylaldiminato complexes [28–30]. The *trans* effect exerted by the chloride ligand is responsible of small lengthening of Ti–Cl bonds in mutual *trans* positions. The Ti–N1(aromatic) distance of 2.190(5) Å agrees with those found in octahedral structures where two pyridine rings are in mutual *trans* positions [31], showing that the phenolate oxygen does not exert, in this case, any *trans* effect. On the other hand, the Ti–N2(imino) distance of 2.169(5) Å displays a significative shortening with respect to those in octahedral Ti-salicylaldiminato derivatives where Ti–N(imino) bond lengths range from 2.24 to 2.31 Å [28–30].

This can be probably due to octahedral distortion pointed out by the narrowing of N1–Ti1–N2 bite angle up to 74.6(2)°. In crystal packing the molecules display an intermolecular Cl2···Cl2 interaction of 3.330(2) Å shorter than the sum of van der Waals radii of 3.50 Å.

In complex **2**, a small *trans* effect can be observed on Zr–Cl bonds. However, in similar complexes, where these distances range from 2.40 to 2.44 Å [29,30,32–34] no systematic lengthening has been observed for Zr1–Cl bonds with Cl ligands in mutual *trans* positions. Likewise in **1** the Zr–N(imino) bond length of 2.329(3) Å shows a significant shortening with respect to similar distances, in the range 2.35–2.39 Å [18] in octahedral Zr-salicylaldiminato derivatives. In this complex the bite angle N1–Zr1–N2 adopts the small value of 71.0(1)°. In the crystal packing the molecules display a short intermolecular Cl3···Cl3 interaction of 3.332(2) Å.

Complex **3** exhibits distances and angles comparable to those of complex **2**. In the crystal packing the molecules of THF act as acceptor of weak C–H···O hydrogen bonds from C10–H and C3–H moieties [C10···O3(x,y,z) = 3.237(6) Å; C3···O2(–x, 1–y, –z) = 3.222(6) Å].

The tridentate ligand in the three complexes undergoes small distortions, probably caused by steric hindrance of *tert*-butyl group, as shown by the rotations of the phenolate group with respect to the quinoline ring of 18.6(2)°, 18.1(1)° and 30.0(1)°, for **1–3**, respectively.

3.4. Olefin polymerizations using complexes **1–3**

Complexes **1–3** were tested as catalysts for ethylene polymerization under a variety of experimental conditions (Table 3).

Only low yields of polyethylene were obtained at 25 °C and 1 atm of monomer pressure (see runs 1–4) using precatalyst **2** in combination with different activators. Reasonable productivities were achieved after activation by methylaluminoxane (MAO) under somehow more drastic conditions, e.g., 50 °C and 6 atm of monomer pressure (see Table 3, runs 5 and 6).

¹³C NMR analyses of the polymers indicate that polyethylenes are linear with virtually no branching.

The polymerization activity increases in the order **3** < **1** < **2**. The molecular weight follows the same trend (see runs 6–8). The

Table 3
Ethylene polymerization: conditions and results

Run	Catalyst	Cocatalyst	Temperature (°C)	Yield (g)	M_n ($\times 10^{-3}$)	M_w ($\times 10^{-3}$)	PDI
1 ^a	2	MAO ^b	25	0.06	–	–	–
2 ^a	2	Dried MAO ^c	25	0.01	–	–	–
3 ^a	2	Al(^t But) ₃ /B(C ₆ F ₅) ₃ ^d	25	trace	–	–	–
4 ^a	2	Al(^t But) ₃ /Ph ₃ CB(C ₆ F ₅) ₄ ^e	25	trace	–	–	–
5 ^f	2	MAO	25	0.12	92	601	6.5
6 ^f	2	MAO	50	2.1	59	194	3.3
7 ^f	3	MAO	50	0.25	13	274	22
8 ^f	1	MAO	50	1.2	44	1077	24

^a General conditions: toluene = 25 mL; precatalyst = 10 μ mol in chlorobenzene (3.3 mM); ethylene pressure = 1 atm; polymerization time = 1 h.

^b MAO = 1 mmol.

^c Dried MAO (1 mmol) obtained by distilling off the solvent by the commercial solution.

^d Al(^tBut)₃ = 0.2 mmol; B(C₆F₅)₃ = 10 μ mol.

^e Al(^tBut)₃ = 0.2 mmol; Ph₃CB(C₆F₅)₄ = 10 μ mol.

^f General conditions: toluene = 75 mL; precatalyst = 30 μ mol; MAO = 3 mmol; ethylene pressure = 6 atm; polymerization time = 1 h.

molecular weight distribution is very broad for **1** and **3**, while it is more narrow for **2**. The very broad PDI values observed suggest a non-single site nature for the catalytic species. This behaviour is frequently observed for non-metallocene catalysts and in particular for catalysts bearing Schiff-base ligands, as reported for bis(phenoxyimine) group 4 metal complexes [35–37]. In fact the imine units of Schiff-base ligands are electrophilic, especially in early transition metal complexes [38]. In particular, the imine moiety can be reduced to an amide functionality by alkylaluminum compounds used as activators [39] or by a

migratory insertion of an alkyl group from the metal centre to the ligand [40]. The reactivity of the imine group could be responsible of the formation of different catalytic species in the polymerization reactions. We studied the reactivity of the imine moiety of the zirconium complex **2** versus migratory insertion of a metal bond alkyl group preparing the corresponding benzyl derivative. The reaction of stoichiometric amount of **LH** and [Zr(CH₂Ph)₄] in benzene-*d*₆ was performed in an NMR tube at 298 K. The ¹H NMR spectrum (Fig. 4) indicated the clean formation of a single species that did not correspond to expected

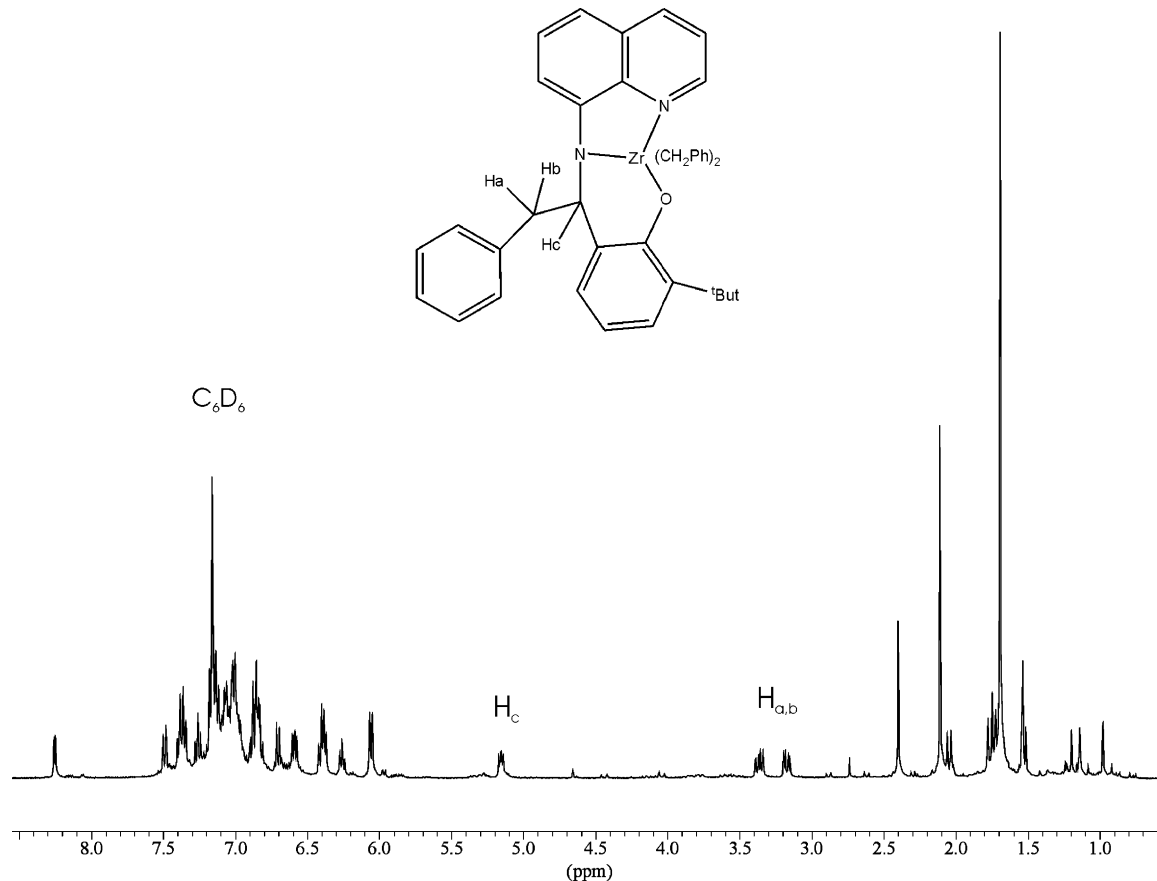


Fig. 4. ¹H NMR spectrum of the reaction product between Zr(CH₂Ph)₄ and ligand **L** at 298 K in benzene-*d*₆.

ZrL(CH₂Ph)₃ complex, but to a pentacoordinate species deriving by a migratory insertion of a benzyl group on the imine group. The characteristic peaks correspond to the formation of a new stereogenic centre at the former imine carbon. The doublet of doublets at 5.15 ppm are attributed to hydrogen at the new chiral amido carbon, the two doublets of doublets (3.34 and 3.18 ppm) are assigned to the diastereotopic hydrogens of the migrated benzyl group [40].

Hydrolysis experiments of the catalytic system formed by **2** and MAO in toluene at 298 K for 10 min gave a mixture of organic compounds in which the most abundant specie is the imine ligand but another compound corresponding to the ligand in which the imine functionality is reduced to generate an amine donor is also evident. Similar results were obtained by protonolysis experiments performed on bis(phenoxyimine) catalysts developed by Fujita and co-workers [35] and binaphthyl-bridged Schiff-base catalysts [41].

These experiments underlined the high reactivity of the imine functionality of the ligand framework of complex **2** and confirmed the possibility that different species are formed in the polymerization mixture.

Complexes **1–3** were also tested as catalysts for the polymerization of propene (see Table 4). In this case, the titanium complex was the most active, while the hafnium complex was substantially inactive.

The polypropylene obtained by **2**-MAO at 50 °C revealed a stereoirregular ([mm] = 34%, [mr] = 39%, [rr] = 27%, see run 12; Table 4) and poorly regioregular microstructure, a considerable amount (about 10%) of regioirregularly arranged monomer units were present, as indicated, e.g., by the broad resonances relative to the adjacent methyl carbons of tail-to-tail arrangements. The same catalytic system resulted inactive at room temperature: only traces of polymer were obtained.

Complex **1**, activated by MAO, afforded, at 50 °C, a poorly stereoregular and regioregular polypropylene ([mm] = 40%, [mr] = 34%, [rr] = 26%, see run 9; Table 4). The same catalytic system, at room temperature (see run 10) afforded a polypropylene with a higher content of isotactic triads ([mm] ~ 50%). A significant amount (~6%) of regioirregularly arranged monomer units is present, as indicated, e.g., by the methyl resonances of the tail–tail units observed between 12.4 and 15.6 ppm from hexamethyldisiloxane. Extraction of the raw polymer with hexane at room temperature resulted in an insoluble, highly isotactic fraction (80%) and a soluble stereoirregular fraction (20%).

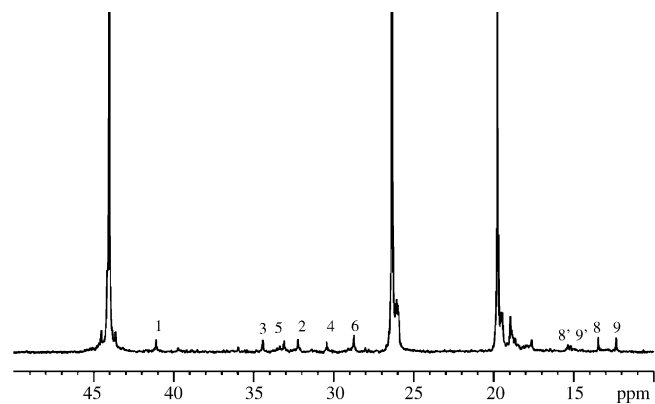


Fig. 5. Aliphatic region of the 100.6 MHz ¹³C NMR spectrum (C₂D₂Cl₄, 100 °C) of the polypropylene obtained from **1**-MAO (run 10).

The presence of macromolecules with different stereoregularities suggests the formation in situ of different catalytic species also in the polymerization of propene as already observed in ethylene polymerizations when the polymerization runs are performed at room or higher temperature. The *n*-hexane-insoluble fraction has a prevalently isotactic structure, with a content of mm triads of 80% (Fig. 5). Pentad analysis of the methyl region of the ¹³C NMR spectrum shows that the most intense resonances detected, in addition to the mmmm signal (19.78 ppm), are those due to the mmmr (19.52 ppm), mmrr (18.96 ppm), mrrm (17.62 ppm) pentads, in approximately 2:2:1 ratio, while the remaining pentad resonances are much less intense. The polymer microstructure therefore mainly consists of blocks of m diads bridged by rr triads, i.e. the microstructure expected for an “enantiomorphic site” mechanism of steric control [42,43].

Detailed analysis of the ¹³C NMR spectrum showed additional less intense and sharp resonances having approximately the same intensity attributable to regioirregularly arranged monomer units. The comparison with literature data [44–46] revealed that the regioinverted monomer units are isolated and that the arrangement of the adjacent methyls is *threo* (see Scheme 2a). In the ¹³C NMR spectrum a group of weak resonances diagnostic of isolated regioirregular monomer units with *erythro* adjacent methyls can be also detected (see Scheme 2b). The *threo/erythro* ratio is about 10:1.

This finding indicates that primary (1,2) and secondary (2,1) insertion of the monomer occur with the same enantioface

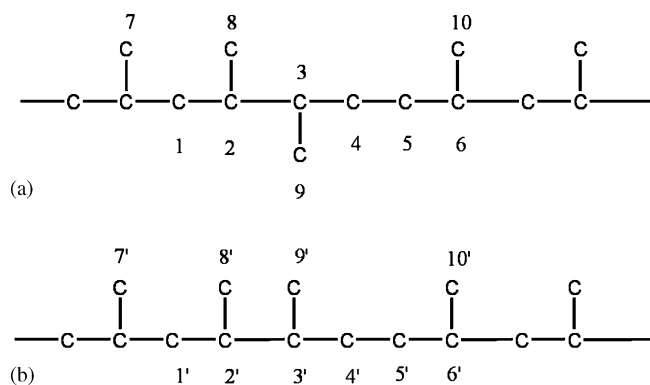
Table 4

Propene polymerization: conditions and results

Run	Catalyst ^a	Temperature (°C)	Yield (g)	[mm%]	[mr%]	[rr%]	Vicinal CH ₃ (%)
9	1	50	0.72	40	34	26	10
10	1	25	0.65	48	29	23	6
11	1	–20	0.10	79	15	6	5
12	2	50	0.10	34	39	27	8
13	2	25	Trace	–	–	–	–
14	3	50	Trace	–	–	–	–
15	3	25	Trace	–	–	–	–

General conditions: toluene = 75 mL; precatalyst = 30 μmol; propene pressure = 6 atm; reaction time = 2 h.

^a Cocatalyst: MAO = 3 mmol.



Scheme 2. Isolated regioinverted propene units with *threo* (a) and *erythro* (b) adjacent methyls in a Fischer projection.

selectivity [47], at variance with the behaviour of isotactic specific metallocene catalysts, such as the classical catalyst based on *rac*-ethylenebis(1-indenyl)dichloro zirconium(IV), which afford a polypropylene having regioirregular sequences with the microstructure of Scheme 2b. Busico et al. recently reported the only precedent of the production of an isotactic polypropylene having isolated regioirregular units in *threo* configuration, [48] using C_1 -symmetric group 4 pyridyl-amine catalysts developed by Dow and Symix [48,49].

A polypropylene sample has also been prepared with **1**-MAO at $-20\text{ }^\circ\text{C}$ (see run 11). In this case the whole raw polymer resulted insoluble in hexane indicating that, at sub-ambient temperature, a more homogeneous polypropylene sample was produced. The ^{13}C NMR spectrum of the polymer showed a polypropylene microstructure identical to that of the *n*-hexane-insoluble fraction obtained by run 10 at room temperature ([mm] $\sim 80\%$, regioinversions = 5%).

In order to shed some light on the nature of the active responsible of the production of a polypropylene with a such peculiar microstructure we carried out some NMR tube experiments to study the reaction between complex **1** and dried MAO (obtained by distilling off the solvent by the commercial solution). Thus, an NMR tube was charged with complex **1** and solid MAO (Al/Ti = 50) in dichloromethane- d_2 at 298 K and ^1H NMR spectra were recorded at intervals. The first spectrum registered after 5 min displayed two different sets of ligand signals indicating the formation of two species in 10/1 ratio. The less abundant species showed resonances coherent with an alkyl titanium complex $\text{LTi}(\text{CH}_3)_3$ (significant resonances, i.e. imine (s, 1H at 9.47 ppm); Ti–Me (s, 3H at 2.40 ppm); $\text{C}(\text{CH}_3)_3$ (s, 9H at 1.69 ppm); Ti–Me (s, 6H at 1.67 ppm)). The most intense resonances were ascribed to the cationic complex $\text{LTi}(\text{CH}_3)_2^+$ (**1a**): noteworthy was a sharp singlet at δ 2.10 ppm, attributed, according to literature data concerning similar phenoxyimine titanium catalysts [39,50], to the six hydrogens of two Ti–CH₃ groups. This attribution was confirmed by ^{13}C NMR spectrum that exhibited an intense and sharp peak at 83.8 δ characteristic of the terminal Ti–Me groups. After 10 min only the cationic $\text{LTi}(\text{CH}_3)_2^+$ species was present (Fig. 6).

Similar NMR experiments (dichloromethane- d_2 at 298 K) were performed to study the reaction between the complex **1**

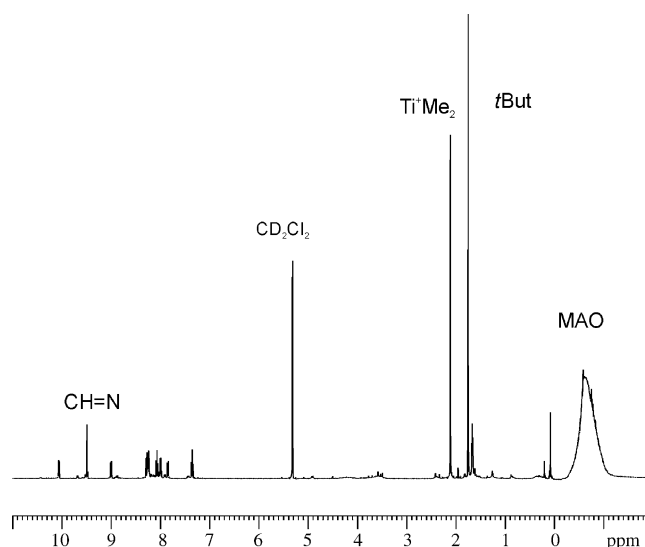


Fig. 6. ^1H NMR spectrum of TiLCl_3 and dried MAO in dichloromethane- d_2 at 298 K.

and $\text{Al}(\text{CH}_3)_3$ (Al/Ti = 50), this is a component of the MAO solution used as activator in the polymerization reactions. ^1H NMR spectra were recorded at intervals. The first spectrum (5 min) showed that complex **1** was quantitatively converted in the single species LTiMe_2^+ (**1a**). After 30 min a second species (**1b**), having the same pattern of the ligand signals of **1a**, appeared. The amount of **1b** increased while that of **1a** decreased with time (**1b** became the most abundant species after 1 h). The identification of complex **1b** was not simple: we excluded that it was an aluminium complex produced by imine ligand exchange with titanium by comparison with literature data [16]. Further, the absence of resonances in the region between 3 and 5 ppm allowed to exclude a reduction of the imine functionality to an amine group.

These studies performed on the titanium complex **1** allowed to affirm: (i) both MAO and $\text{Al}(\text{CH}_3)_3$ were able to generate a cationic alkyl species which could be responsible of the polymerization activity and (ii) in presence of $\text{Al}(\text{CH}_3)_3$ a second unidentified species was formed in which the ligand skeleton of the titanium precatalyst was not modified. In conclusion the investigations about the reactivity of the imine functionality of ligand framework in zirconium (**2**) and titanium (**1**) complexes suggest that different species can be generated depending on the nature of the metal centre and on the reaction conditions. In particular, under mild experimental conditions (sub-ambient temperature) a more homogeneous catalytic system could be generated.

While the structure of the true active complexes deriving from the reaction of complexes **1** with MAO cannot be clearly defined at this moment, the production of an isotactic polypropylene with such an unusual microstructure suggests that the active species are not trivial complexes deriving by complete ligand removal. We are currently studying these catalysts to continue to investigate the structure of the active specie and rationalize the effects of structural modifications of the ligand architecture on the polypropylene microstructure.

Supplementary material

Crystallographic data (excluding structure factors) for the three structures reported in the present paper have been deposited at the Cambridge Crystallographic Data Centre and allocated the deposition numbers CCDC 282669–282671. These data can be obtained free of charge via <http://www.ccdc.ac.uk/conts/retrieving.html> or on application to CCDC, Union Road, Cambridge CB2 1EZ, UK [fax: +44 1223 336033, e-mail: deposit@ccdc.cam.ac.uk].

Acknowledgment

The work has been funded by the MURST PRIN-2004 (prot. 2004030307_3).

References

- [1] G.J.P. Britovsek, V.C. Gibson, D.F. Wass, *Angew. Chem.* 38 (1999) 428.
- [2] V.C. Gibson, S.K. Spitzmesser, *Chem. Rev.* 103 (2003) 283–316.
- [3] Y. Suzuki, H. Terao, T. Fujita, *Bull. Chem. Soc. Jpn.* 76 (2003) 1493–1517 (and references therein).
- [4] P.A. Cameron, V.C. Gibson, C. Redshaw, J.A. Segal, A.J.P. White, D.J. Williams, *J. Chem. Soc., Dalton Trans.* (2002) 415 (and references therein).
- [5] D.J. Jones, V.C. Gibson, S.M. Green, P.J. Maddox, *Chem. Commun.* (2002) 1038 (and references therein).
- [6] R.K. O'Reilly, V.C. Gibson, A.J.P. White, D.J. Williams, *J. Am. Chem. Soc.* 125 (2003) 8450 (and references therein).
- [7] H. Nitta, D. Yu, M. Kudo, A. Mori, S. Inoue, *J. Am. Chem. Soc.* 114 (1992) 7969–7975.
- [8] A.M. El-Hendawy, A.H. Alkubaisi, A.E.-G. El-Kourasy, M.M. Shanab, *Polyhedron* 12 (1993) 2343–2350.
- [9] W.A. Herrmann, B. Cornils, *Angew. Chem. Int. Ed. Engl.* 36 (1997) 1049–1067.
- [10] J. Du Bois, C.S. Tomooka, E.M. Carreira, M.W. Day, *Angew. Chem. Int. Ed. Engl.* 36 (1997) 1645–1647.
- [11] T. Fujita, Y. Tohi, M. Mitani, S. Matsui, J. Saito, M. Nitabar, K. Sugi, H. Makio, T. Tsutsui, Mitsui Chemicals Inc., European Patent, EP 0874005 (1998).
- [12] S. Matsui, Y. Tohi, M. Mitani, J. Saito, H. Makio, H. Tanaka, M. Nitabar, T. Nakano, T. Fujita, *Chem. Lett.* (1999) 1065.
- [13] M. Mitani, J. Saito, S.I. Ishii, Y. Nakayama, H. Makio, Y. Matsukawa, S. Matsui, J.I. Mohri, R. Furuyama, Y. Terao, H. Bando, H. Tanaka, T. Fujita, *Chem. Rec.* 4 (2004) 137–158.
- [14] J. Tian, G.W. Coates, *Angew. Chem. Int. Ed.* 39 (2000) 3626.
- [15] J. Tian, P.D. Hustad, G.W. Coates, *J. Am. Chem. Soc.* 123 (2001) 5134.
- [16] H. Makio, T. Fujita, *Bull. Chem. Soc. Jpn.* 78 (2005) 52–66 (and references therein).
- [17] J. Saito, M. Mitani, J. Mohri, Y. Yoshida, S. Matsui, S. Ishii, S. Kojoh, N. Kashiwa, T. Fujita, *Angew. Chem. Int. Ed.* 40 (2001) 2918.
- [18] M. Mitani, J. Mohri, Y. Yoshida, J. Saito, S. Ishii, K. Tsuru, S. Matsui, R. Furuyama, T. Nakano, H. Tanaka, S. Kojoh, T. Matsugi, N. Kashiwa, T. Fujita, *J. Am. Chem. Soc.* 124 (2002) 3327.
- [19] T.R. Younkin, E.F. Connor, J.I. Henderson, S.K. Friedrich, R.H. Grubbs, D.A. Bansleben, *Science* 287 (2000) 460.
- [20] S. Xiuli, H. Weiqiu, W. Cong, T. Yong, Z. Yuliang, X. Chun-An, US Patent, US2005004331 (2005).
- [21] Z. Otwinowski, W. Minor, in: C.W. Carter, R.M. Sweet (Eds.), *Methods in Enzymology*, vol. 276, part A, Academic Press, London, 1997, p. 307.
- [22] R.H. Blessing, *Acta Crystallogr. Sect. A* 51 (1995) 33.
- [23] A. Altomare, M.C. Burla, M. Camalli, G.L. Casciaro, C. Giacovazzo, A. Guagliardi, A.G. Moliterni, G. Polidori, R. Spagna, *SIR97, J. Appl. Crystallogr.* 32 (1999) 115.
- [24] G.M. Sheldrick, *SHELX-97, Program for Crystal Structure Refinement*, University of Göttingen, Germany, 1997.
- [25] M. Nardelli, *J. Appl. Crystallogr.* 28 (1995) 659.
- [26] L.J. Farrugia, *J. Appl. Crystallogr.* 32 (1999) 837.
- [27] M.N. Burdett, C.K. Johnson, *ORTEP III, Report ORNL-6895*, Oak Ridge National Laboratory, Oak Ridge, TN, 1996.
- [28] D.A. Pennington, D.L. Hughes, M. Bochmann, S.J. Lancaster, *J. Chem. Soc., Dalton Trans.* (2003) 3480–3482.
- [29] R.K.J. Bott, M.D. Hughes, L. Schormann, M. Bochmann, S.J. Lancaster, *J. Organomet. Chem.* 665 (2003) 135–149.
- [30] D.A. Pennington, W. Clegg, S.J. Coles, R.W. Harrington, M.B. Hursthouse, D.L. Hughes, M.J. Light, M. Schormann, M. Bochmann, S.J. Lancaster, *J. Chem. Soc., Dalton Trans.* (2005) 561.
- [31] K. Hensen, A. Lemke, M. Bolte, *Acta Crystallogr. Sect. C* 55 (1999) 863.
- [32] D. Zhang, G.-X. Jin, *Appl. Catal.: Gen.* 262 (2004) 85.
- [33] C.L. Nygren, M.E.T. Bragg, J.F.C. Turner, *Acta Crystallogr. Sect. C* 60 (2004) 4.
- [34] C.E.F. Rickard, M.W. Glenny, A.J. Nielsen, *Acta Crystallogr. Sect. E* 59 (2003) 183.
- [35] S. Matsui, M. Mitani, J. Saito, Y. Tohi, H. Makio, N. Matsukawa, Y. Takagi, K. Tsuru, M. Nitabar, T. Nakano, H. Tanaka, N. Kashiwa, T. Fujita, *J. Am. Chem. Soc.* 123 (2001) 6847.
- [36] Y. Tohi, H. Makio, S. Matsui, M. Onda, T. Fujita, *Macromolecules* 11 (2003) 523.
- [37] D. Liu, S. Wang, H. Wang, W. Chen, *J. Mol. Catal. A* (2006) 246.
- [38] M.J. Scott, S.J. Lippard, *Organometallics* 16 (1997) 5857.
- [39] H. Makio, T. Fujita, *Macromol. Symp.* 213 (2004) 221.
- [40] P.D. Knight, P.N. O'Shaughnessy, I.J. Munsolv, B.S. Kimberley, P. Scott, *J. Organomet. Chem.* 683 (2003) 103.
- [41] M. Lamberti, M. Consolmagno, M. Mazzeo, C. Pellicchia, *Macromol. Rapid Commun.* 26 (2005) 1866.
- [42] C. Wolsgruber, G. Zannoni, E. Rigamonti, A. Zambelli, *Makromol. Chem.* 176 (1975) 2765.
- [43] R.A. Shelden, T. Fueno, T. Tsunstsugu, J. Furukawa, *J. Polym. Sci. Part B* 3 (1965) 23.
- [44] A. Zambelli, P. Locatelli, E. Rigamonti, *Macromolecules* 12 (1979) 156–159.
- [45] A. Grassi, A. Zambelli, L. Resconi, E. Albizzati, R. Mazzocchi, *Macromolecules* 21 (1988) 617.
- [46] V. Busico, R. Cipullo, C. Polzone, G. Talarico, J.C. Chadwich, *Macromolecules* 36 (2003) 2616.
- [47] G. Guerra, L. Cavallo, G. Moscardi, M. Vacatello, P. Corradini, *J. Am. Chem. Soc.* 116 (1994) 2988.
- [48] V. Busico, R. Cipullo, G. Talarico, J.C. Stevens, *Abstract of Papers of EUPOC 2003* (2003) 81.
- [49] J.C. Stevens, D. Vanderlende, Dow Chemical Co., PCT Patent WO 03040201 (2003).
- [50] K.P. Bryliakov, E.A. Kravtsov, D.A. Pennington, S.J. Lancaster, M. Bochman, H. Britzinger, E.P. Talsi, *Organometallics* 24 (2005) 5660.